

# Molecular Distillation of Petroleum Residues and Physical-Chemical Characterization of Distillate Cuts Obtained in the Process

Lamia Zuñiga Liñan,\* Melina Savioli Lopes,<sup>†</sup> and Maria R. Wolf Maciel<sup>†</sup>

Separation Process Development Laboratory (LDPS), School of Chemical Engineering, University of Campinas, UNICAMP, P.O. Box 6066, CEP 13083-970, Campinas-SP, Brazil

Nádson M. Nascimento Lima<sup>†</sup> and Rubens Maciel Filho<sup>†</sup>

Optimization, Project and Advanced Control Laboratory (LOPCA), School of Chemical Engineering, University of Campinas, UNICAMP, P.O. Box 6066, CEP 13083-970, Campinas-SP, Brazil

Marcelo Embiruçu<sup>†</sup>

Programa de Engenharia Industrial, Escola Politécnica, Universidade Federal da Bahia (UFBA), Salvador, Brazil

Lílian C. Medina<sup>†</sup>

Centro de Pesquisas e Desenvolvimento da Petrobras (CENPES/Petrobras), Rio de Janeiro, Brazil

---

Molecular distillation is presented as an alternative technique for the separation of petroleum residues. The technique was used to obtain 13 heavy petroleum cuts from three atmospheric residues (ARs) at 673.15 K and above. The cuts present initial and final boiling points between (673.15 and 951.15) K. To evaluate the efficiency of the technique, chemical characterization of residues and distillate cuts, which included SARA fractionation, <sup>13</sup>C NMR, elemental composition, and density and viscosity analysis, was performed. In addition, extended true boiling point curves of crude oils by simulated distillation and by molecular distillation were compared. An increase in the viscosity and in the density was observed in all cuts with an increased molecular distillation temperature. Such behavior demonstrates that highly polar components that have a high structural complexity, such as resins and asphaltenes, are concentrated at the higher temperatures of the process. A sensitivity analysis of these two properties, together with the temperature, showed that viscosity and density decreased with increased temperature. On the other hand, the thermal expansion coefficient values obtained were equivalent to those reported in literature for petroleum products. Furthermore, a complete characterization of crude oils was made using the molecular distillation process to extend the true boiling point (TBP) curves.

---

## 1. Introduction

Petroleum residues are petroleum products that cannot be removed by means of atmospheric distillation,<sup>1</sup> and this material is generated in two different columns during the refining process. An atmospheric residue (AR) is a term used to describe the material at the bottom of the atmospheric distillation column which has an atmospheric equivalent boiling point (AEBP) from 673.15 K upward (673.15 K+). A vacuum residue (VR) forms at the bottom of the vacuum distillation column and presents an AEBP from 813.15 K on (813.15 K+).<sup>2</sup>

Heavy petroleum cuts present molecules containing over 25 carbon atoms (C<sub>25</sub>). They also present structural complexity, high molecular weight, and high polarity, which increases the boiling temperature, the density, and the viscosity.<sup>1</sup>

The demand for basic as well as specialized petrochemicals increases every day. This requires greater quantities of raw materials and higher quality to obtain products to meet

consumption demands. The petroleum industry has responded to satisfying such demands either by presenting process improvements or by looking for alternatives to offer the highest quality petrochemical commodities and materials.

Along with the decrease in the supply of petrochemical naphtha from the increase in the production of heavy crude oil with aromatic/naphthenic features, developing and improving technologies that lead to the production of heavy oil derivatives with a greater added-value, which result in a more thorough petroleum characterization, are also a challenge.

The fractionating of the crude oils is usually carried out through conventional distillation methods, ASTM D2892 and ASTM D5236.<sup>3,4</sup> The ARs are fractionated by the ASTM D5236 method, but this is limited to temperatures below 838 K. For higher temperatures a well-established method does not exist, although high-temperature simulated distillation (HTDS) by gas chromatography (GC) is well-adapted and used to extend the true boiling point curves (TBP).<sup>5–7</sup>

To obtain a more efficient separation from petroleum residues, thus diminishing the risk of thermal degradation and reaching an enhanced performance of the cuts produced, a method based on molecular distillation was implemented by the Separation

\* Corresponding author. Tel.: + 55 19 35213971; fax number: +55 19 35213910; e-mail: lazuli@feq.unicamp.br.

<sup>†</sup> E-mail: melinaslopes@yahoo.com.br; wolf@feq.unicamp.br; nadson@feq.unicamp.br; maciel@feq.unicamp.br; embiruçu@ufba.br; lmedina@petrobras.com.br.

Process Development Laboratory (LDPS) and the Optimization, Project, and Advanced Control Laboratory (LOPCA) at the Chemical Engineering School of UNICAMP and the Research Center of Petrobras-Brazil (CENPES/Petrobras). This method extended the TBP curves of crude oils at temperatures higher than the ones achieved by conventional distillation methods. The technique is based upon short path distillation in high vacuum conditions (0.1 Pa), which represents a smaller operational temperature and a smaller exposure time of the distilled liquid on the heated surface.<sup>8</sup> In addition, research carried out and in progress at LDPS/LOPCA/UNICAMP-Petrobras<sup>2,8</sup> has demonstrated the potential of the technique for use in industrial fractionation of heavy residues. Knowledge of the viscosity, density, and chemical composition of petroleum products is important to define their commercial values and future applications. The main characteristic of high-boiling-point petroleum fractions is directly related to the major presence of compounds such as resins and asphaltenes, which constitute the highest polar fractions of these products. Their macrostructures are probably responsible for the high viscosity of this material.<sup>1</sup> Furthermore, more detailed structural characterizations by using liquid chromatography (SARA fractionation), elementary and oil analysis, nuclear magnetic resonance (NMR), infrared spectroscopy (IR), and others are necessary to improve process routes, to upgrade these materials, and to add value to them.

The objective of this work is to carry out the separation of three atmospheric petroleum residues within the process temperature range from (439.15 to 603.15) K, using the molecular distillation technique in the laboratory. As a result, 13 distillate cuts and 13 residues of molecular distillation were generated. To evaluate the efficiency of the technique, chemical characterization, including SARA fractionation, <sup>13</sup>C NMR, and elemental composition analysis of the ARs and the distilled cuts, was performed. An analysis of viscosity and density behavior with temperature, at the range (313.15 to 373.15) K, was also considered. Sensitivity analysis carried out for viscosity–temperature and density–temperature behavior enabled the definition of the thermal expansion coefficient of this type of mixture. Additionally, the TBP curves of three crude oils were constructed and compared with the extended TBP curves by HTDS and the molecular distillation process. The uncertainties of the results presented here are within the expected range of values, according to the requirements of the experimental methods.

## 2. Experimental Section

**2.1. Molecular Distillation.** To fractionate ARs, a falling film molecular distillator KDL 5-Mini Pilot Plant/UIC-GmbH was used. The basic design of the equipment is a short-path distillation unit, as shown in Figure 1: a vertical double-jacketed cylinder (evaporator) with a cooled and centered internal condenser and a rotating roller wiper basket (composed of four rollers) with an external drive. The equipment also has a feed device with a gear pump, rotating carousels that hold discharge sample collectors for the products from the molecular distillation process (each carousel consists of six collectors that can be positioned and moved by the operator without interrupting the distillation process), a set of vacuum pumps with an in-line low-temperature cold trap, and four heating units.<sup>8</sup> The short-path distillation unit has a concave configuration, that is, the evaporation occurs on the inner surface of the outer cylinder and the condensation at the outer surface of the inner cylinder.<sup>9</sup> The roller wipers have a length of 0.165 m measured from the top of evaporator. They are positioned on the internal surface

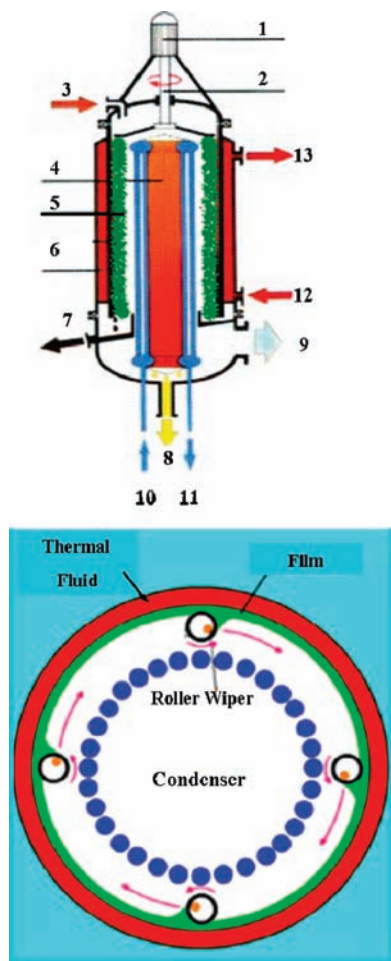


**Figure 1.** Inner configuration of falling film molecular distillator and front view of heated evaporator used for the separation of ARs 673.15 K+ of AL and JES crude oils. 1 and 2, engine and agitation blades; 3, feeding; 4, condenser; 5, falling film; 6, evaporator; 7, residue output; 8, distillate output; 9, vacuum system; 10 and 11, cooling fluid; 12 and 13, thermal fluid. This figure is an adaptation of original design on <http://www.UIC-GmbH.de/>.

of the evaporator, and their principal function is to homogenize the film formed and to enable easier heat transfer from the inner layers (in contact with the evaporator wall) to the film surface. The molecular distillation process occurs in steady-state; thus, the AR is continuously fed, and two product flows are continuously generated: distillate cuts and residue of molecular distillation. As soon as all temperatures (feed temperature, evaporator temperature, condenser temperature, and product temperatures) and the vacuum pressure are reached, the wiper system is started. Then, the rotating gear pump feeds the sample at a constant rate onto a rotating distribution plate from a heat feed container that, for these petroleum residues, must be at 353.15 K. Centrifugal gravity forces distribute the material onto the inner surface of the evaporator in the form of a very thin film, with a thickness which will depend on the mixture viscosity and feeding flow. Volatile components vaporize from the film and condense on the cooled inner condenser. The separation takes place in four basic stages: transport of evaporated compounds from the liquid mixture to the film surface, distillation of the mixture from the film surface, transport of evaporated molecules through distillation gap (space between evaporator and condenser), and condensation of evaporated molecules. The most volatile components which are not condensed are collected in the cold trap. Distillate cuts and residue from molecular distillation are collected separately in

**Table 1. Physical-Chemical Characterization and Molecular Distillation Operational Conditions for the Atmospheric Residues ARAL, ARJES, and ARBA<sup>a</sup>**

$P_{DM}/\text{Pa}$	0.1						
$T_F/\text{K}$	353.15						
$T_C/\text{K}$	363.15						
$Q_F/\text{L}\cdot\text{h}^{-1}$	0.5						
$R_A/\text{rpm}$	250						
feed to molecular distillator	TDM/K	API	C	H	N	S	H/C
ARAL	439.15 to 603.15	12.9	0.869	0.122	0.007	0.008	1.91
ARJES	483.15 to 598.15	11.6	0.874	0.115	0.006	0.007	1.94
ARBA	483.15 to 598.15	12.9	0.860	0.112	0.010	0.008	1.91

<sup>a</sup>  $P_{DM}$  is the pressure of the molecular distillation process;  $T_F$  is the feed temperature;  $T_C$  is the condenser temperature;  $Q_F$  is the feed flow rate;  $R_A$  is the agitation rate in the evaporator; and TDM is the range of temperature used in the molecular distillation process; C, H, N, and S are the carbon, hydrogen, nitrogen, and sulfur compositions in mass fraction, respectively; H/C is the hydrogen-to-carbon atomic ratio.

reservoir cylinders assembled in two carousels. The heating fluid (JULABO thermaloil) circulating through the double-jacketed cylinder provides the heat for the wall evaporator. The cooling fluid (water at a constant temperature) cools the condensing cylinder. The vacuum pressure (0.1 Pa) in the distillator is set by a rotary vane pump and a diffusion pump. The residence time depends on the molecular distillation conditions, especially on the evaporator temperature. It ranges between (5 to 8) min. In this work a collecting time of 15 min was used, after which the feed to the evaporator was interrupted to change the temperature of the evaporator (TDM). During this transition the feed temperature and the condenser temperature were kept constant. Table 1 describes the molecular distillation conditions established to split the three ARs. These are identified by their theoretical names: ARAL (atmospheric residue of crude oil AL), ARJES (atmospheric residue of crude oil JES), and ARBA (atmospheric residue of crude oil BA). The initial boiling point (IBP) of the most volatile components of the mixtures is 673.15 K. The final boiling point (FBP) of the mixtures is unknown or even infinite, as the heaviest components may never vaporize at all.<sup>10</sup> Table 1 also shows the temperature ranges used for the molecular distillation, TDM, the API gravity of the cuts, the elemental composition of residues expressed in mass fraction of carbon (C), hydrogen (H), nitrogen (N), and sulfur (S), and the hydrogen-to-carbon atomic ratio (H/C).

**2.2. Analysis of Viscosity and Density of Distillate Cuts.** Viscosities and densities of the generated distillate cuts at test temperature  $T_{\text{test}}$  from (313.15 to 373.15) K were obtained using an Anton Paar Stabinger SVM 3000 viscometer. The instrument and its operation have been described elsewhere.<sup>11</sup> The piece of equipment is comprised of two measuring systems: the coaxial cylinder measuring system used to measure the viscosity of the sample, and the digital density analyzer, which uses a U-shaped oscillating sample tube and a system for electronic excitation and frequency counting to measure the density of the sample. During the test, the sample is introduced into the measuring cells, which are at a closely controlled and known temperature. The dynamic viscosity is determined from the equilibrium rotational speed of the inner cylinder under the influence of the shear stress of the sample and an eddy current brake, in conjunction with adjustment data. The density is determined by the oscillation frequency of the U-tube in conjunction with adjustment data.<sup>11</sup> The kinematic viscosity is calculated by dividing the dynamic viscosity by the density.

To control the temperature, a copper block surrounds both the viscosity and the density measuring devices. A thermoelec-

tric heating and cooling system ensures the stability of the copper block within  $\pm 0.005$  K around the set temperature at the position of the viscosity cell over the whole temperature range. The factory calibration ensures a temperature standard uncertainty ( $k = 2$ ; 95 % confidence level) of no more than 0.03 K over the range of (288.15 to 373.15) K.<sup>11</sup> The long-term stability of the Pt-100 platinum probe ensures less than 0.01 K temperature drift per year.

Standard uncertainties in the measurements of viscosity and density were determined in accordance with the Guidelines for Evaluating and Expressing the Uncertainty of NIST Measurement Results, using eq 1:

$$\mu(x_i) = s(\bar{X}_i) = \left[ \frac{1}{n(n-1)} \sum_{k=1}^n (X_{i,k} - \bar{X}_i)^2 \right]^{1/2} \quad (1)$$

where  $\mu(x_i)$  is the standard uncertainty of measurement result  $x_i$ , expressed in  $\text{m}^2\cdot\text{s}^{-1}$  for the viscosity measurements and in  $\text{kg}\cdot\text{m}^{-3}$  for the density measurements,  $s(\bar{X}_i)$  is the standard deviation of the average of the measuring results  $\bar{X}_i$ ,  $n$  is the total number of measurements, and  $X_{i,k}$  is the value of the measured result. Calculated standard uncertainties are presented in Table A.1 in Appendix A for all of the distillate cuts studied. The kinematic viscosities were measured with repeatability at a 95 % confidence level. The values were calculated using the expressions:  $0.000943X$  at 313.15 K and  $0.0003473(X + 5)$  at 373.15 K,<sup>11</sup> where  $X$  is the average of the measuring results. Table A.2 in Appendix A shows the detailed calculations. According to the requirements of the method, the uncertainty ( $k = 2$ ; 95 % confidence level) of the density values should have a maximum of  $0.1 \text{ kg}\cdot\text{m}^{-3}$ , and the repeatability (95 % confidence level) should have a maximum of  $0.297 \text{ kg}\cdot\text{m}^{-3}$  at 313.15 K and  $0.332 \text{ kg}\cdot\text{m}^{-3}$  at 373.15 K. To calibrate the instrument, the detailed procedure of the manufacturer of the apparatus described in the reference manual, firmware version 2.0.8, was followed.

**2.3. Chemical Characterization.** The chemical characterization analysis: SARA fractionation, <sup>13</sup>C NMR, and elemental composition were developed by the CENPES/Petrobras Laboratories. SARA fractionation was used to determine the proportion in mass fraction of saturated, aromatic, resin, and asphaltene compounds presented in the samples of ARs and the distillate cuts obtained. The technique used was the thin layer chromatography (TLC) with field ionization detector (FID). The instrument and its operation are described in the ASTM D4124 method.<sup>12</sup> The aromatic and aliphatic carbon proportion (in mass fraction) of the studied mixtures were defined by <sup>13</sup>C NMR according to the ASTM D5292 method.<sup>13</sup> The chemical element composition analysis of the mixtures obtained from the molecular distillation of petroleum ARs was carried out using a Perkin-Elmer elementary analyzer, model 2400. The instrument and its operation are described in ASTM D4530 and ASTM D4294 for the determination of carbon residue (micromethod) and sulfur concentration, respectively.<sup>14,15</sup> The repeatability of carbon residue  $r_{\text{CR}}$  and sulfur concentration  $r_{\text{SC}}$  measurements vary according to the percentage of carbon residue and to the concentration of sulfur in the sample, as shown in eqs 2 and 3, respectively:

$$r_{\text{CR}} = 3.161 \cdot 10^{-2} (\% \text{ micromethod carbon residue} + 3) \quad (2)$$

$$r_{SC} = 0.4347 - X^{0.6446} \quad (3)$$

where  $X$  is the sulfur concentration in  $\text{mg}\cdot\text{kg}^{-1}$  of total sulfur. For sulfur concentration the required repeatability is  $2.6 \text{ mg}\cdot\text{kg}^{-1}$  for  $X = 16.0 \text{ mg}\cdot\text{kg}^{-1}$  (0.0016 %) and  $440 \text{ mg}\cdot\text{kg}^{-1}$  for  $X = 46000 \text{ mg}\cdot\text{kg}^{-1}$  (4.6 %).<sup>15</sup> Table A.3 in Appendix A shows the detailed calculations.

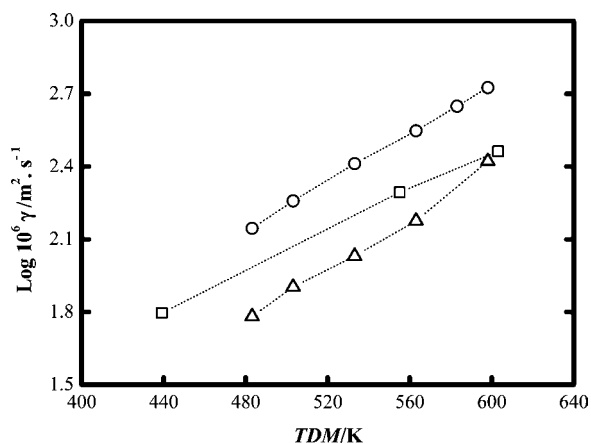


**Figure 2.** Kinematic viscosity profiles  $\gamma$  for test temperature  $T_{\text{test}} = 333.15$  K of distilled cuts regarding the molecular distillation temperature TDM = (439.15 to 603.15) K.  $\square$ , AL cuts;  $\circ$ , JES cuts;  $\triangle$ , BA cuts.

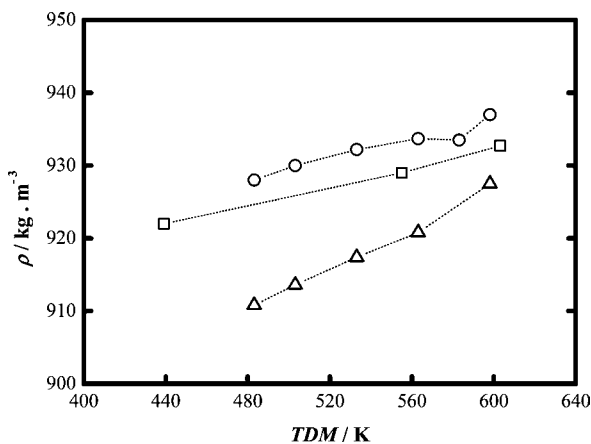


**Figure 3.** Density profiles for test temperature  $T_{\text{test}} = 333.15$  K  $\rho_{60}$  of distillate cuts regarding the molecular distillation temperature TDM = (439.15 to 603.15) K.  $\square$ , AL cuts;  $\circ$ , JES cuts;  $\triangle$ , BA cuts.

**Table 2. Chemical Element Composition and Thermal Expansion Coefficient of the Distillate Cuts Obtained through the Molecular Distillation Process<sup>a</sup>**

crude oil	TDM	T	C	H	N	S	H/C	API	$k$
	K	K							$\text{kg}^2\cdot\text{m}^{-6}\cdot\text{K}^{-1}$
AL	439.15	673.15 to 781.15	0.868	0.118	0.003	0.005	1.74	17.0	-1170
	555.15	673.15 to 882.15	0.865	0.117	0.004	0.006	1.82	16.3	-1160
	603.15	673.15 to 951.15	0.868	0.117	0.005	0.006	1.84	15.9	-1150
	483.15	673.15 to 810.15	0.877	0.127	<0.003	0.005	1.77	17.2	-1130
JES	503.15	673.15 to 827.15	0.870	0.128	<0.003	0.005	1.78	16.3	-1140
	533.15	673.15 to 857.15	0.870	0.127	<0.003	0.005	1.80	16.0	-1140
	563.15	673.15 to 893.15	0.869	0.120	<0.003	0.006	1.81	15.7	-1100
	598.15	673.15 to 943.15	0.881	0.127	<0.003	0.006	1.84	15.3	-1110
	483.15	673.15 to 810.15	0.862	0.119	<0.003	0.006	1.79	19.5	-1120
BA	503.15	673.15 to 827.15	0.862	0.120	<0.003	0.006	1.80	19.2	-1120
	533.15	673.15 to 857.15	0.859	0.118	<0.003	0.006	1.81	18.4	-1130
	563.15	673.15 to 893.15	0.860	0.119	0.003	0.007	1.82	17.9	-1140
	598.15	673.15 to 943.15	0.865	0.118	0.003	0.007	1.83	17.1	-1150

<sup>a</sup> TDM is the temperature of molecular distillation process;  $T$  is the range of boiling points of the cuts obtained by molecular distillation; C, H, N, and S are the carbon, hydrogen, nitrogen, and sulfur compositions in mass fraction, respectively; H/C is the hydrogen-to-carbon atomic ratio; API is API gravity, and  $k$  is the thermal expansion coefficient of the distillate cuts.

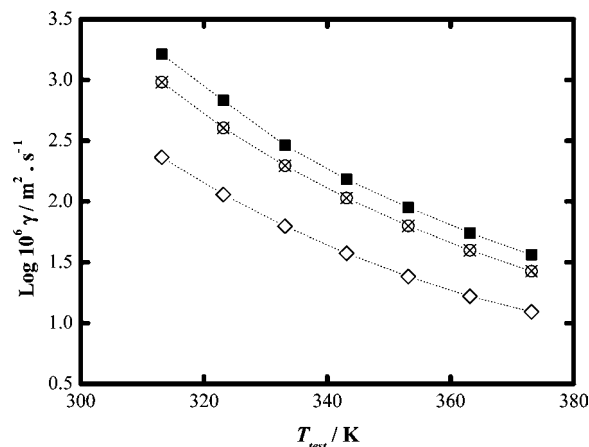


**Figure 4.** Kinematic viscosity profiles  $\gamma$  regarding the test temperature  $T_{\text{test}} = (313.15 \text{ to } 373.15)$  K for AL distillate cuts obtained by molecular distillation.  $\diamond$ , cut (673.15 to 781.15) K;  $\otimes$ , cut (673.15 to 882.15) K;  $\blacksquare$ , cut (673.15 to 951.15) K.

### 3. Results and Discussion

Figures 2 and 3 present the behavior of the kinematic viscosity  $\gamma$  and of the density at  $333.15$  K  $\rho_{60}$  with the TDM for the cuts obtained from the molecular distillation of petroleum residues. It can be seen that both the viscosity and the density increase as the molecular distillation temperature is increased. If the fact that the high viscosity and polarity of heavy petroleum cuts is related to the presence of macro-structures typical of resins and asphaltenes,<sup>1</sup> it is possible to affirm that the fractioning of petroleum residues through molecular distillation enables the generation of cuts with a remarkable difference in the composition of such compounds, which are present in a greater proportion as the distillation temperature is increased. On the other hand, it can be observed that the JES petroleum distillate cuts present greater viscosity and density values, which indicates that such cuts are formed by molecules of a higher complexity than the other petroleum cuts. Provided that viscosity is increased as the API gravity of the cuts decreases,<sup>10</sup> these results can be justified because the API gravities of the JES petroleum distillate cuts are the smallest ones, as shown in Table 2.

Figures 4 to 6 and 7 to 9 show the kinematic viscosity and density variation profiles as a function of the test temperature for the petroleum cuts obtained. The figures demonstrate the outstanding influence of the test temperature and of the distillate cut composition in kinematic viscosity. This confirms the fact

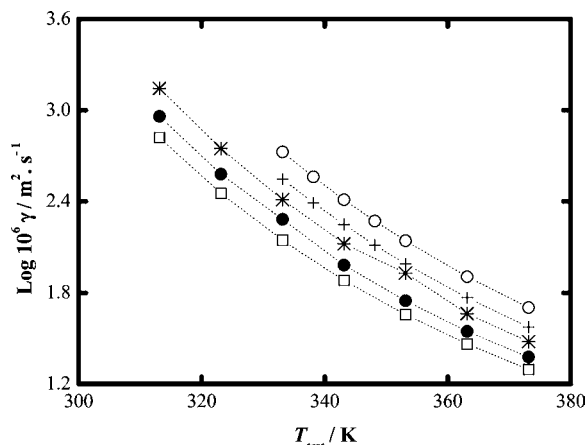


**Figure 5.** Kinematic viscosity profiles  $\gamma$  regarding the temperature  $T_{\text{test}} = (313.15 \text{ to } 373.15) \text{ K}$  for JES distilled cuts obtained by molecular distillation.  $\square$ , cut (673.15 to 810.15) K;  $\bullet$ , cut (673.15 to 827.15) K;  $*$ , cut (673.15 to 857.15) K;  $+$ , cut (673.15 to 893.15) K;  $\circ$ , cut (673.15 to 943.15) K.

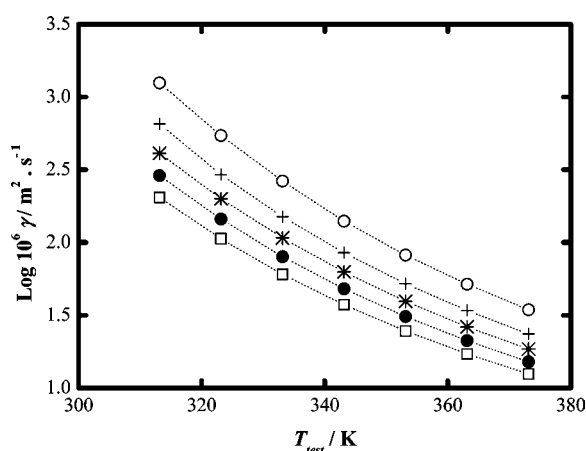


**Figure 6.** Kinematic viscosity profiles  $\gamma$  regarding the test temperature  $T_{\text{test}} = (313.15 \text{ to } 373.15) \text{ K}$  for BA distillate cuts obtained by molecular distillation.  $\square$ , cut (673.15 to 810.15) K;  $\bullet$ , cut (673.15 to 827.15) K;  $*$ , cut (673.15 to 857.15) K;  $+$ , cut (673.15 to 893.15) K;  $\circ$ , cut (673.15 to 943.15) K.

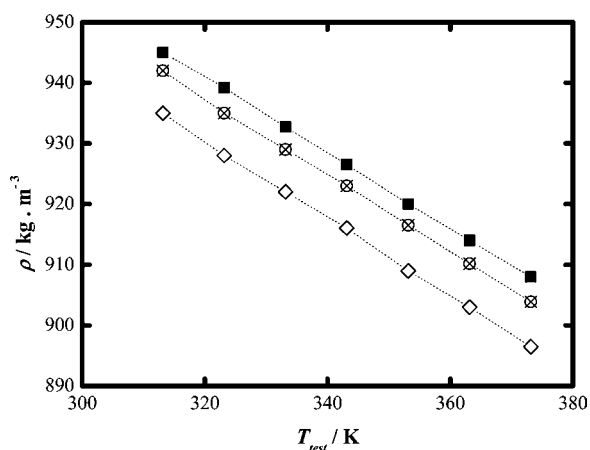


**Figure 7.** Density profiles regarding the test temperature  $T_{\text{test}} = (313.15 \text{ to } 373.15) \text{ K}$   $\rho$  for AL distillate cuts obtained by molecular distillation.  $\diamond$ , cut (673.15 to 781.15) K;  $\boxtimes$ , cut (673.15 to 882.15) K;  $\blacksquare$ , cut (673.15 to 951.15) K.

that the viscosity of the cuts is increased as the molecular distillation temperature rises. It is possible to see from the figures that the cuts with greater boiling temperature ranges, which are obtained at the highest molecular distillation temperatures, are

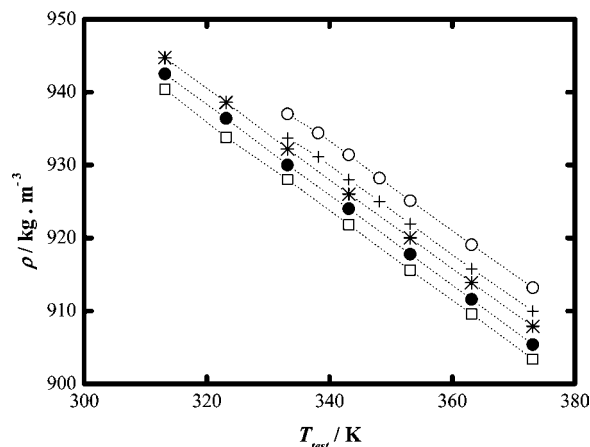


**Figure 8.** Density profiles regarding the test temperature  $T_{\text{test}} = (313.15 \text{ to } 373.15) \text{ K}$   $\rho$  for JES distillate cuts obtained by molecular distillation.  $\square$ , cut (673.15 to 810.15) K;  $\bullet$ , cut (673.15 to 827.15) K;  $*$ , cut (673.15 to 857.15) K;  $+$ , cut (673.15 to 893.15) K;  $\circ$ , cut (673.15 to 943.15) K.

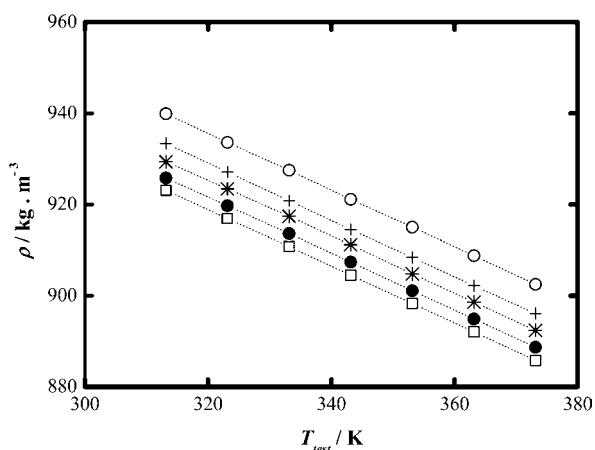


**Figure 9.** Density profiles regarding the test temperature  $T_{\text{test}} = (313.15 \text{ to } 373.15) \text{ K}$   $\rho$  for BA distillate cuts obtained by molecular distillation.  $\square$ , cut (673.15 to 810.15) K;  $\bullet$ , cut (673.15 to 827.15) K;  $*$ , cut (673.15 to 857.15) K;  $+$ , cut (673.15 to 893.15) K;  $\circ$ , cut (673.15 to 943.15) K.

the ones that present greater viscosity values. For the density measurements a small variation in this property with the test temperature and with the molecular distillation temperature can be seen. While a difference in distillation temperature represents a variation in cut composition, such a variation has no significant effect on the density value, as this property depends on the volumetric expansion and contraction of the sample due to the effect of temperature, which is also small for cuts in the liquid phase.

Figure 10 shows the thermal expansion coefficient values at 333.15 K,  $\alpha_{60}$ , of the distillate cuts obtained from experimental density data at test temperature. A Fortran 90 computer code was developed to calculate this property, based on API methods 11.1.5.2, 11.1.5.3, and 11.1.5.4.<sup>16–18</sup> It can be observed that the coefficients show little change with the molecular distillation temperature and that they oscillate around a central value (the average value  $\alpha_{60\text{av}} = 6.66 \cdot 10^{-4} \text{ K}^{-1}$ ). The coefficient of thermal expansion is directly related to the thermal volumetric coefficient  $k$ , that is, related to the inclination of the square of the density versus temperature curves.<sup>19</sup> Figures 7 to 9 show that for distillate cuts all of the curves are parallel to each other, so it is difficult to observe any deviation between them. In Table 2 the values of the thermal volumetric coefficient for the generated cuts are shown for each molecular distillation temperature. The  $k$  values vary just a little between the distillate cuts, and such

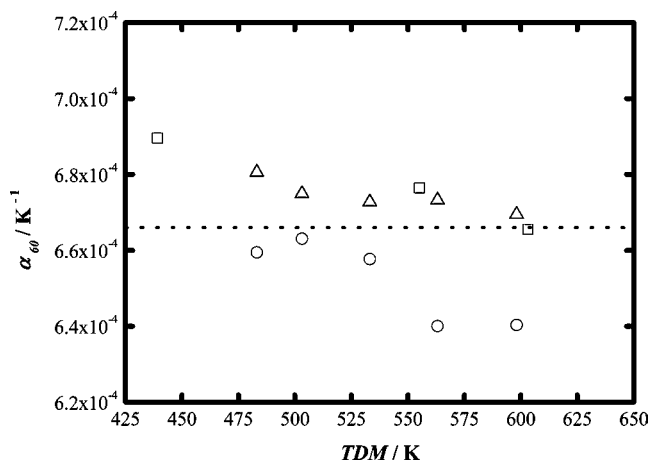


**Figure 10.** Coefficients of thermal expansion at 333.15 K  $\alpha_{60}$  of the petroleum cuts regarding the molecular distillation temperature TDM.  $\square$ , AL cuts;  $\circ$ , JES cuts;  $\triangle$ , BA cuts;  $\dots$ , average value of thermal expansion coefficient at 333.15 K  $\alpha_{60av} = (6.66 \cdot 10^{-4} \text{ K}^{-1})$ .

values are very close to the ones reported in the literature<sup>19</sup> for petroleum products ( $-1100 \text{ kg}^2 \cdot \text{m}^{-6} \cdot \text{K}^{-1}$ ).

Table 2 lists the range of boiling point  $T$ , the density API, and the chemical element composition of the distillate cuts obtained at each temperature of the molecular distillation TDM. The AEBP of the IBP and the FBP of the cuts were calculated with the FRAMOL correlation, which establishes an equivalence between the molecular distillation temperature (high vacuum) and the atmospheric pressure temperature. Details about the formulation of the FRAMOL correlation have been described elsewhere.<sup>8</sup> Table 2 shows values that are typical of the heavy oil cuts obtained through conventional distillation. An increase in the concentration of carbon, hydrogen, nitrogen, and sulfur can be seen as the boiling temperature range is increased. The cuts present a low nitrogen concentration when compared to the concentration of this element in the AR. This indicates that such a compound has been separated from the distillate cuts and concentrated in the molecular distillation residues where much more complex molecules predominate with enhanced aromaticity and polarity and which evaporate at temperatures

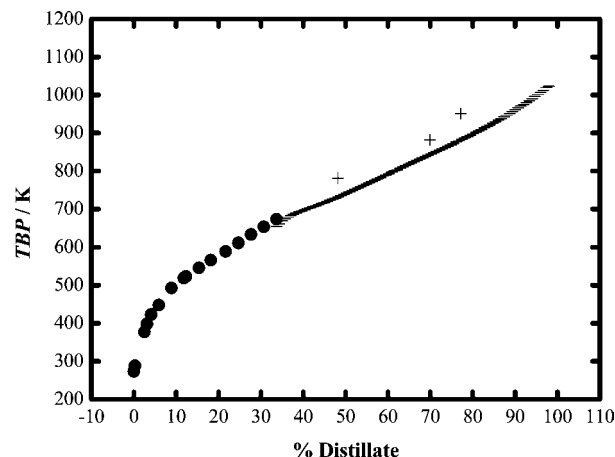


**Figure 11.** TBP curve in mass by ASTM D2892 and ASTM D5236 methods, boiling range distribution by HTDS, and extension of TBP curve by molecular distillation process for AL crude oil.  $\bullet$ , TBP curve of crude oil generated by ASTM D2892 method;  $\square$ , HTDS curve of ARAL residue;  $+$ , extended TBP by molecular distillation process of distillate cuts at (673.15 to 781.15) K, (673.15 to 882.15) K, and (673.15 to 951.15) K.

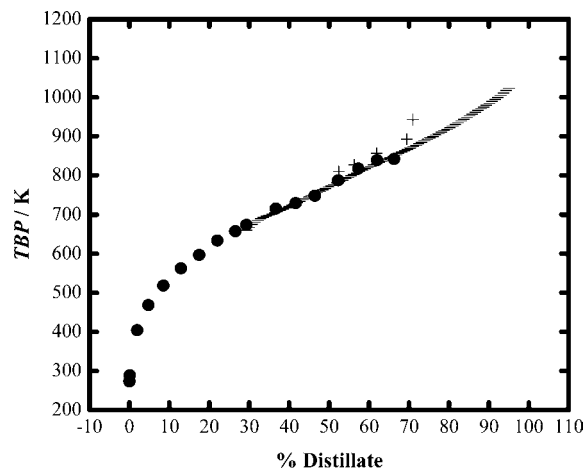
higher than 951.15 K. Also, it is observed that the aromaticity (H/C ratio) of the distillate cuts increases with the TDM used in the process.

Table 3 shows the proportion of saturated compounds: paraffins with molecular structure  $\text{C}_n\text{H}_{2n+2}$ ; aromatic compounds: resin compounds: polyaromatic compounds, especially kerogen<sup>20</sup> and asphaltene compounds: polyaromatic hydrocarbons, especially dibenzothiophene ( $\text{C}_{12}\text{H}_8\text{S}$ , CAS No. 132-65-0)<sup>10</sup> and 2,3-benzocarbazole ( $\text{C}_{16}\text{H}_{11}\text{N}$ , CAS No. 243-28-7)<sup>10</sup> present in the studied samples. A high concentration of asphaltenes in the ARs was observed when compared with the concentration of these compounds in the distillate cuts. The concentration of the saturated compounds and aromatic compounds are enriched in the distillate cuts as the TDM rises, while the concentration of the resins and asphaltenes decreases. The results of  $^{13}\text{C}$  NMR indicated a major proportion of aliphatic carbon (quaternary carbons, CH,  $\text{CH}_2$ , and  $\text{CH}_3$ ) than aromatic carbon in the

**Table 3.** Chemical Characterization by SARA Fractionation and NMR of the Atmospheric Residues ARAL, ARJES, and ARBA and the Distillate Cuts Obtained through Molecular Distillation Process<sup>a</sup>

sample	SARA fractionation				$^{13}\text{C}$ NMR	
	saturated	aromatic	resins	asphaltene	aromatic carbon	aliphatic carbon
Feed to Molecular Distillator						
ARAL	0.20	0.43	0.27	0.10	0.23	0.77
ARJES	0.17	0.41	0.29	0.13	0.23	0.77
ARBA	0.19	0.42	0.28	0.11	0.24	0.76
Distillation Cuts of AL Crude Oil						
673.15 to 781.15	0.53	0.40	0.05	0.02	0.22	0.78
673.15 to 882.15	0.43	0.46	0.08	0.03	0.22	0.78
673.15 to 951.15	0.57	0.28	0.11	0.03	0.23	0.77
Distillation Cuts of JES Crude Oil						
673.15 to 810.15	0.47	0.44	0.09	0.01	0.21	0.79
673.15 to 827.15	0.46	0.44	0.09	0.01	0.21	0.79
673.15 to 857.15	0.41	0.44	0.14	0.01	0.21	0.79
673.15 to 893.15	0.40	0.44	0.15	0.01	0.22	0.78
673.15 to 943.15	0.36	0.43	0.19	0.02	0.22	0.78
Distillation Cuts of BA Crude Oil						
673.15 to 810.15	0.40	0.49	0.09	0.02	0.20	0.80
673.15 to 827.15	0.35	0.54	0.10	0.01	0.19	0.81
673.15 to 857.15	0.34	0.48	0.17	0.01	0.19	0.81
673.15 to 893.15	0.32	0.53	0.13	0.02	0.20	0.80
673.15 to 943.15	0.31	0.50	0.15	0.04	0.21	0.79

<sup>a</sup> Composition of SARA fractionation and  $^{13}\text{C}$  NMR analysis are expressed in mass fraction.



**Figure 12.** TBP curve in mass by ASTM D2892 and ASTM D5236 methods, boiling range distribution by HTDS, and extension of TBP curve by molecular distillation process for JES crude oil. ●, TBP curve of crude oil generated by ASTM D2892 and ASTM D5236 methods; ■, HTDS curve of ARJES residue; +, extended TBP by molecular distillation process of distillate cuts at (673.15 to 810.15) K, (673.15 to 827.15) K, (673.15 to 857.15) K, (673.15 to 893.15) K, and (673.15 to 943.15) K.

distillate cuts, which demonstrate that through the molecular distillation an efficient fractionation of heavy residues is achieved.

Figures 11 and 12 show the TBP curves of the AL and JES crude oils. These curves were obtained by conventional distillation methods ASTM D2892 and ASTM D5236. These figures also show the boiling range distribution by HTDS of the ARAL and ARJES residues. Moreover, the yields at FBP of the distillate cuts of AL and JES crude oils obtained by molecular distillation were also plotted. The TBP and HTDS curves were provided by CENPES/Petrobras Laboratories. The percentage of distillate accumulated in mass (distillate percentage from crude) of the three distillate cuts of the AL crude oil and of the five distillate cuts of JES crude oils were used to extend the TBP curves of the crude oils by molecular distillation. The results show that the yields of distillate obtained by the molecular distillation process are comparable with those defined by the conventional distillation process. In the molecular distillation process the process temperature is expected to be equivalent to the FBP of the generated cut. As observed in Figures 11 and 12, this expectation is confirmed in the analyzed cuts because the FBP of the cuts generated by molecular distillation can be seen to be quite close to those defined by HTDS. In Table 4 the small differences between the boiling range distribution by HTDS and the FBP defined for each distillate cut generated by molecular distillation process indicate that the extended TBP curve defined by the latter is representative of crude oils. Furthermore, using this technique, the TBP curves were extended above 838.15 K (951.15 K for the JES crude oil), which represents a yield of over (70 to 80) % in mass, a very important result when compared with the (30 to 60) % in mass obtained by conventional methods. This represents a gain of about (20 to 30) % in distillate. Molecular distillation is therefore an efficient way to separate these complex residues to obtain greater improvement and a more complete characterization of the crude oils, and it also has significant advantages when compared with the conventional HTDS separation method because the products of the distillation are generated; a preliminary deasphalting step of the sample<sup>1</sup> is not necessary, and the operation conditions

**Table 4.** Final Boiling Point (FBP) Defined by HTDS and by Molecular Distillation Process for the Distillate Cuts of AL and JES Crude Oils<sup>a</sup>

crude oil	T/K	FBP <sub>HTDS</sub> /K	FBP <sub>DM</sub> /K	$\Delta T$ /K
AL	673.15 to 781.15	788.15	781.15	7.00
	673.15 to 882.15	896.05	882.15	13.90
	673.15 to 951.15	931.05	951.15	-20.10
JES	673.15 to 810.15	837.65	810.15	27.50
	673.15 to 827.15	839.25	827.15	12.10
	673.15 to 857.15	867.05	857.15	9.90
	673.15 to 893.15	892.95	893.15	-0.20
	673.15 to 943.15	965.65	943.15	22.50

<sup>a</sup>  $T$  is the range of boiling points of the cuts obtained by molecular distillation; FBP<sub>HTDS</sub> and FBP<sub>DM</sub> are the final boiling points of the cut defined by HTDS and by molecular distillation, respectively;  $\Delta T$  is the difference between the final boiling points (FBP<sub>HTDS</sub> - FBP<sub>DM</sub>) for the distillate cuts.

of molecular distillation process generate distillate cuts with an AEBP above 873 K without risks of thermal degradation. Table A.1 in Appendix A summarizes the results of the viscosity and density measurements. It shows that the uncertainties of the measurements are within the expected range of values. The uncertainty of density measurements for each test temperature do not exceed the maximum value required by the method ( $0.1 \text{ kg} \cdot \text{m}^{-3}$ ), which indicates the correct operation of the piece of equipment. Moreover, Tables A.1 and A.2 in Appendix A show that the major uncertainties and repeatability of viscosity measurements are found for the higher viscosities. As observed in Table A.3 in Appendix A, the repeatability of the carbon residue and sulfur concentration measurements are also within the constraints of the ASTM D4530 and ASTM D4294 methods, respectively. The repeatability of the sulfur concentration measurements varies according to the sulfur concentration, but within the range established by the method:  $106 \text{ mg} \cdot \text{kg}^{-1}$  for a sulfur concentration of  $5000 \text{ mg} \cdot \text{kg}^{-1}$  (corresponding to a sulfur concentration of 0.005 for the distillate cut at (673.15 to 810.15) K of JES crude oil, in Table 2) and  $143 \text{ mg} \cdot \text{kg}^{-1}$  for a sulfur concentration of  $8000 \text{ mg} \cdot \text{kg}^{-1}$  (sulfur concentration of 0.008 of AR at 673.15 K + of AL crude oil, in Table 1).

#### 4. Conclusions

The efficiency of molecular distillation to fractionate heavy petroleum residues was verified through the physical-chemical analysis of distillate cuts obtained from the fractionation of ARs (673.15 K+) of three heavy crude oils. In general terms, an increase in the viscosity and density of the cuts could be observed as the molecular distillation temperature was increased. This can be explained by a higher distillation temperature which produces distillate cuts which have a higher proportion of compounds with more complex molecular structures and with typical features of resins and asphaltene. On the other hand, the analysis of the chemical element composition showed a greater concentration of carbon, hydrogen, nitrogen, and sulfur in the cuts obtained at the highest distillation temperatures. In addition, expected petroleum product values for the thermal expansion coefficient as well as for the thermal volumetric coefficient were found in the distillate cuts produced.

The comparative analysis of the extended TBP curves by HTDS and by the molecular distillation process demonstrated that this alternative method is appropriate to extend the TBP curves to temperatures above those of the conventional methods, overcoming the limitations that are common in the

HTDS method, and enable a (20 to 30) % improvement in distillate and a more complete characterization of the crude oils. The uncertainty and repeatability analysis demonstrated that the viscosity, density, and chemical element composition measurements were generated with the correct operation of the equipment.

#### Appendix A

#### Uncertainty and Repeatability of Kinematic Viscosity, Density, and Chemical Element Composition Measurements for the Samples Analyzed

Experimental data of kinematic viscosity and density of the distillate cuts obtained by molecular distillation process are listed in Table A.1 for each test temperature. The predicted uncertainty for both properties is also given in detail. Table A.2 shows the repeatability (at 95 % confidence level) for kinematic viscosity results at (313.15 and 373.15) K. The repeatability was determined in accordance with the ASTM D7042 standard test

**Table A.2. Summary of the Repeatability of Kinematic Viscosity Measurements<sup>a</sup>**

crude oil	$T$	$10^6 r (95\%)_{40}$	$10^6 r (95\%)_{100}$
	K	$\text{m}^2 \cdot \text{s}^{-1}$	$\text{m}^2 \cdot \text{s}^{-1}$
AL	673.15 to 781.15	0.218	0.006043
	673.15 to 882.15	0.905	0.01103
	673.15 to 951.15	1.534	0.01443
JES	673.15 to 810.15	0.622	0.008595
	673.15 to 827.15	0.860	0.01394
	673.15 to 857.15	1.314	0.01220
	673.15 to 893.15	0.491 <sup>b</sup>	0.01479
BA	673.15 to 943.15	0.742 <sup>b</sup>	0.501
	673.15 to 810.15	0.192	0.006074
	673.15 to 827.15	0.271	0.006991
	673.15 to 857.15	0.386	0.008175
	673.15 to 893.15	0.616	0.009900
	673.15 to 943.15	1.177	0.01372

<sup>a</sup>  $T$  is the range of boiling points of the cuts obtained by molecular distillation,  $r (95\%)_{40}$  and  $r (95\%)_{100}$  are the repeatability at 95 % confidence level of the kinematic viscosities measured at (313.15 and 373.15) K, respectively. <sup>b</sup> This value was calculated by linear extrapolation from the results obtained at (333.15 and 373.15) K.

**Table A.1. Summary of the Uncertainty of Kinematic Viscosity and Density Results<sup>a</sup>**

crude oil	$T$	$T_{\text{test}}$	$10^6 \gamma$	$10^{-3} \rho$	$10^6 \mu(\gamma)$	$10^{-3} \mu(\rho)$	crude oil	$T$	$T_{\text{test}}$	$10^6 \gamma$	$10^{-3} \rho$	$10^6 \mu(\gamma)$	$10^{-3} \mu(\rho)$		
	K	K	$\text{m}^2 \cdot \text{s}^{-1}$	$\text{kg} \cdot \text{m}^{-3}$	$\text{m}^2 \cdot \text{s}^{-1}$	$\text{kg} \cdot \text{m}^{-3}$		K	K	$\text{m}^2 \cdot \text{s}^{-1}$	$\text{kg} \cdot \text{m}^{-3}$	$\text{m}^2 \cdot \text{s}^{-1}$	$\text{kg} \cdot \text{m}^{-3}$		
AL	673.15 to 781.15	313.15	230.87	0.93	0.01	0.00	673.15 to 943.15	333.15	531.3	0.9370	0.4	0.0002			
		323.15	113.825	0.93	0.006	0.00		338.15	364.2	0.93	0.2	0.00			
	333.15	62.54	0.92225	0.09	0.00006	343.15	257.4	0.93135	0.1	0.00005					
	343.15	37.540	0.91595	0.004	0.00006	348.15	186.7	0.93	0.3	0.00					
	353.15	24.214	0.90965	0.002	0.00006	353.15	138.4	0.92	0.3	0.00					
	363.15	16.632	0.90335	0.001	0.00006	363.15	80.639	0.92	0.006	0.00					
	373.15	12.4	0.867	0.5	0.04	373.15	50.55	0.91325	0.03	0.00005					
	673.15 to 882.15	313.15	959.8	0.94	2.1	0.00	BA	673.15 to 810.15	313.15	203.7	0.92310	0.3	0.00005		
		323.15	402.5	0.93	0.4	0.00			323.15	105.930	0.92	0.005	0.00		
		333.15	196.6	0.93	0.1	0.00			333.15	60.49	0.91080	0.01	0.00005		
		343.15	106.56	0.92315	0.03	0.00006			343.15	37.378	0.9045	0.002	0.0001		
		353.15	62.894	0.91695	0.002	0.00006			353.15	24.645	0.8983	0.001	0.00001		
		363.15	39.812	0.9107	0.004	0.00			363.15	17.154	0.89	0.001	0.00		
		373.15	26.76	0.9046	0.00	0.00			373.15	12.49	0.88	0.00	0.00		
		673.15 to 951.15	313.15	1627.6	0.94555	0.1			0.00006	673.15 to 827.15	313.15	287.7	0.9258	0.2	0.0001
			323.15	676.6	0.9392	0.2			0.00		323.15	144.50	0.91970	0.02	0.00005
			333.15	290.0	0.91955	0.7			0.01		333.15	80.036	0.91	0.006	0.00
	343.15		151.7	0.9078	0.4	0.001	343.15	48.118	0.91		0.006	0.00			
	353.15		89.1	0.9202	0.1	0.00	353.15	30.996	0.90110		0.006	0.00005			
	363.15		55.2	0.9141	0.4	0.00	363.15	21.148	0.89490		0.002	0.00005			
	373.15		36.58	0.908	0.01	0.00	373.15	15.13	0.89		0.00	0.00			
JES	673.15 to 810.15		313.15	659.5	0.94	0.4	0.00	673.15 to 857.15	313.15		409.51	0.9294	0.09	0.0001	
			323.15	283.7	0.93380	0.3	0.00009		323.15		199.24	0.9234	0.09	0.0002	
			333.15	139.64	0.92795	0.01	0.00005		333.15		107.32	0.92	0.03	0.00	
		343.15	76.18	0.92	0.02	0.00	343.15		62.838	0.91120	0.002	0.00005			
		353.15	45.355	0.92	0.008	0.00	353.15		39.461	0.9848	0.002	0.0002			
		363.15	29.060	0.90955	0.001	0.00005	363.15		26.345	0.89860	0.001	0.00005			
		373.15	19.748	0.90345	0.001	0.00005	373.15		18.539	0.89240	0.001	0.00005			
		673.15 to 827.15	313.15	911.6	0.94	0.5	0.00		673.15 to 893.15	313.15	653.21	0.93	0.09	0.00	
			323.15	379.50	0.93635	0.09	0.00005			323.15	291.95	0.9271	0.02	0.0002	
			333.15	181.2	0.9299	0.5	0.0001			333.15	150.0	0.9208	0.3	0.0002	
343.15	96.07		0.92395	0.02	0.00005	343.15	85.610	0.91		0.006	0.00				
353.15	55.98		0.91775	0.01	0.00005	353.15	52.19	0.90840		0.00	0.00005				
363.15	35.1485		0.91155	0.0005	0.00005	363.15	34.1070	0.90220		0.0005	0.00005				
373.15	23.484		0.90545	0.001	0.00005	373.15	23.505	0.89610		0.001	0.00005				
673.15 to 857.15	313.15		1393.2	0.9447	2.5	0.0001	673.15 to 943.15	313.15		1249.0	0.9399	2.0	0.0001		
	323.15		559.2	0.93855	0.2	0.00005		323.15		542.8	0.9336	0.6	0.0002		
	333.15		258.0	0.9322	0.2	0.0002		333.15		264.0	0.9275	0.2	0.0002		
	343.15	132.66	0.92605	0.09	0.00005	343.15		139.61	0.92	0.02	0.00				
	353.15	75.18	0.91995	0.02	0.00005	353.15		81.982	0.92	0.006	0.00				
	363.15	46.08	0.91	0.01	0.00	363.15		51.69	0.90880	0.03	0.00005				
	373.15	30.114	0.91	0.006	0.00	373.15		34.5130	0.90250	0.0005	0.00005				
	673.15 to 893.15	313.15	352.4	0.9337	0.1	0.0001									
		338.15	246.37	0.93	0.07	0.00									
		343.15	176.96	0.92805	0.04	0.00005									
348.15		130.11	0.92	0.00	0.00										
353.15		97.800	0.92	0.006	0.00										
363.15		58.60	0.91585	0.01	0.00005										
373.15		37.578	0.90995	0.002	0.00005										

<sup>a</sup>  $T$  is the range of boiling points of the cuts obtained by molecular distillation,  $T_{\text{test}}$  is the temperature of the test,  $\gamma$  is the kinematic viscosity of the cuts,  $\rho$  is the density of the cuts, and  $\mu(\gamma)$  and  $\mu(\rho)$  are the standard uncertainties of viscosity results and density results, respectively.



**Table A.3. Summary of the Repeatability of Carbon Residue and Sulfur Concentration Measurements<sup>a</sup>**

crude oil	$T$	$r_{CR}$	$r_{SC}$
	K	%	mg·kg <sup>-1</sup>
AL	673.15 +	2.842	143
	673.15 to 781.15	2.838	109
	673.15 to 882.15	2.829	118
	673.15 to 951.15	2.838	120
JES	673.15 +	2.857	132
	673.15 to 810.15	2.867	106
	673.15 to 827.15	2.845	108
	673.15 to 857.15	2.845	112
	673.15 to 893.15	2.542	114
BA	673.15 to 943.15	2.880	118
	673.15 +	2.813	143
	673.15 to 810.15	2.820	115
	673.15 to 827.15	2.820	117
	673.15 to 857.15	2.810	124
	673.15 to 893.15	2.813	126
	673.15 to 943.15	2.829	127

<sup>a</sup>  $T$  is the range of boiling point of the cuts obtained by molecular distillation, and  $r_{CR}$  and  $r_{SC}$  are the repeatabilities of the carbon residue and sulfur concentration measurements covering the requirements of the methods ASTM D4530 and ASTM D4294, respectively.

method: (0.000943X) at 313.15 K and (0.0003473X) at 373.15 K, where X stands for the average of the measured value. Table A.3 shows the repeatability for carbon residue and sulfur concentration calculated for the ARs fed to the molecular distillation process and for the distillate cuts obtained by the process, covering the full scope and requirements of methods ASTM D4530 and ASTM D4294.

### Acknowledgment

The authors would like to thank CENPES/Petrobras for the performance of tests with the chemical characterization analysis: SARA fractionation, <sup>13</sup>C NMR, and elemental composition of distillate cuts involving the AL, JES, and BA oils.

### Literature Cited

- (1) Merdrignac, I.; Espinat, D. Physicochemical Characterization of Petroleum Fractions: the State of the Art. *Oil Gas Sci. Technol.* **2007**, *62*, 7–32.
- (2) Maciel Filho, R.; Batistella, C. B.; Sbaite, P.; Winter, A.; Vasconcelos, C. J. G.; Wolf Maciel, M. R.; Gomes, A.; Medina, L.; Kunert, R. Evaluation of Atmospheric and Vacuum Residues using Molecular Distillation and Optimization. *Petrol. Sci. Technol.* **2006**, *24*, 275–283.
- (3) American Society for Testing and Materials - ASTM D2892. *Standard Test Method for Distillation of Crude Petroleum (15-Theoretical Plate Column)*; ASTM International: West Conshohocken, PA, 2005.
- (4) American Society for Testing and Materials - ASTM D5236. *Standard Test Method for Distillation of Heavy Hydrocarbon Mixtures (Vacuum Potstill Method)*; ASTM International: West Conshohocken, PA, 2003.
- (5) Villalanti, D. C.; Raia, J. C.; Maynard, J. B. *Encyclopedia of Analytical Chemistry; High-Temperature Simulated Distillation Applications in Petroleum Characterization*; John Wiley & Sons, Ltd.: Chichester, 2000.
- (6) Ferreira, A. A.; Radler, F. A. Destilação Simulada na Indústria do Petróleo. *Quim. Nova* **2005**, *28*, 478–482.
- (7) Brandão, U. Uso da Técnica de Destilação simulada de Alta Temperatura para Extrapolação da Curva de Ponto de Ebulição Verdadeiro de Petróleos. *Bol. Tec. PETROBRAS* **2002**, *45*, 343–349.
- (8) Sbaite, P.; Batistella, C. B.; Winter, A.; Vasconcelos, C. J. G.; Wolf Maciel, M. R.; Maciel Filho, R.; Gomes, A.; Medina, L.; Kunert, R. True Boiling Point Extended Curve of Vacuum Residue through Molecular Distillation. *Petrol. Sci. Technol.* **2006**, *24*, 265–274.
- (9) Xubin, Z.; Chunjian, X.; Ming, Z. Modeling of Falling Film Molecular Distillator. *Sep. Sci. Technol.* **2005**, *40*, 1371–1386.
- (10) Riazí, M. R. *Characterization and Properties of Petroleum Fractions*; ASTM International Standards Worldwide: West Conshohocken, PA, 2004.
- (11) American Society for Testing and Materials - ASTM D7042. *Standard Test Method for Dynamic Viscosity and Density of Liquids by Stabinger Viscometer (and the Calculation of Kinematic Viscosity)*; ASTM International: West Conshohocken, PA, 2004.
- (12) American Society for Testing and Materials - ASTM D4124. *Standard Test Method for Separation of Asphalt into Four Fractions*; ASTM International: West Conshohocken, PA, 2009.
- (13) American Society for Testing and Materials - ASTM D5292. *Standard Test Method for Aromatic Carbon Contents of Hydrocarbon Oils by High Resolution Nuclear Magnetic Resonance Spectroscopy*; ASTM International: West Conshohocken, PA, 2009.
- (14) American Society for Testing and Materials - ASTM D4530. *Standard Test Method for Determination of Carbon Residue (Micro Method)*; ASTM International: West Conshohocken, PA, 2007.
- (15) American Society for Testing and Materials - ASTM D4294. *Standard Test Method for Sulfur in Petroleum and Petroleum Products by Energy Dispersive X-ray Fluorescence Spectrometry*; ASTM International: West Conshohocken, PA, 2008.
- (16) API. *Manual of petroleum measurement standards, Section 1, Method 11.1.5.2.*; API Publishing Services: Washington, DC, 2004.
- (17) API. *Manual of petroleum measurement standards, Section 1, Method 11.1.5.3.*; API Publishing Services: Washington, DC, 2004.
- (18) API. *Manual of petroleum measurement standards, Section 1, Method 11.1.5.4.*; API Publishing Services: Washington, DC, 2004.
- (19) O'Donnell, R. J. Predict Thermal Expansion of Petroleum. *Hydrocarb. Process.* **1980**, *59*, 229–231.
- (20) Speight, J. G. Petroleum Asphaltene Part 1. Asphaltene, Resins and the Structure of Petroleum. *Oil Gas Sci. Technol.* **2004**, *59*, 467–477.

Received for review December 23, 2009. Accepted July 6, 2010. The authors would like to thank the financial support offered by CAPES, FAPESP, CNPq, and FINEP.

JE9010807